Mechanism of Assembly of the Tyrosyl Radical–Diiron(III) Cofactor of *E. coli* Ribonucleotide Reductase. 3. Kinetics of the Limiting Fe^{2+} Reaction by Optical, EPR, and Mössbauer Spectroscopies

J. Martin Bollinger, Jr.,[§,⊥] Wing Hang Tong,[§] Natarajan Ravi,[†,∥] Boi Hahn Huynh,[*,†] Dale E. Edmondson,[*,‡] and JoAnne Stubbe[*,§]

Contribution from the Departments of Chemistry and Biology, Massachusetts Institute of Technology, Cambridge, Massachusetts 02139, and the Departments of Physics and Biochemistry, Emory University, Atlanta, Georgia 30322

Received January 13, 1994[⊕]

Abstract: The R2 subunit of *E. coli* ribonucleotide reductase contains a tyrosyl radical–diiron(III) cofactor which assembles spontaneously when apo R2 is mixed with Fe^{2+} and O_2. The kinetic/spectroscopic characteristics of this assembly reaction were previously shown to depend on the Fe^{2+}/apo R2 ratio (Bollinger, J. M., Jr. et al. *Science* **1991**, *253*, 292–298). In the case of the reaction carried out with limiting Fe^{2+} (Fe^{2+}/apo R2 = 2.0–2.4), two intermediates were proposed to accumulate. On the basis of its broad absorption feature at 560 nm, the first intermediate was suggested to contain a μ-peroxodiferric cluster. The one-electron oxidation of tyrosine 122 by this cluster was postulated to generate the second intermediate, which was proposed to contain the tyrosyl radical (•Y122) and the diferric radical species (Ravi, N. et al. *J. Am. Chem. Soc.*, first of three papers in this issue; Bollinger, J. M., Jr. et al. *J. Am. Chem. Soc.* **1991**, *113*, 6289–6291). In this study, stopped-flow absorption, rapid freeze–quench electron paramagnetic resonance, and rapid freeze–quench Mössbauer spectroscopies have been used to characterize in detail the kinetics of the assembly reaction carried out with limiting Fe^{2+}. The time course of development and decay of the 560 nm absorption transient, and the quantities of diferric radical species, •Y122, and product diferric cluster as functions of time, are consistent with the proposal that the 560 nm absorbing species generates •Y122. The data indicate, in contrast to our previous hypothesis, that the 560 nm absorbing species is not iron based. It is proposed, instead, that the species is a tryptophan radical cation produced by the one-electron oxidation of W48. The results of this study are consistent with our previous proposal that Fe(IV) intermediates are not involved in generation of •Y122.

Introduction

The tyrosyl radical–diferric cluster cofactor in the R2 subunit of *E. coli* ribonucleotide reductase assembles spontaneously when apo R2 is mixed with Fe^{2+} and O_2.[1] In previous work,[2,3] kinetic and spectroscopic evidence guided us in proposing a mechanism for this reconstitution reaction (see Scheme 1 in paper 1 of this series[4]). The hypothetical mechanism involves a partition between two reaction pathways, which follow different fates of the common intermediate, **I**. The partition ratio depends on the initial ratio of Fe^{2+}/R2, which determines the availability of the "extra" reducing equivalent (previously demonstrated to be required for electron balance[5–7]). The preceding paper[7] reports results from reconstitution of R2 with excess Fe^{2+} (Fe^{2+}/R2 ≥ 5) and presents evidence for the accumulation of an intermediate diferric radical species (***X***),[4] which kinetic evidence implicates as the immediate precursor to the product cofactor. In addition, the paper establishes the quantitative agreement among data obtained by stopped-flow absorption (SF-Abs), rapid freeze-quench EPR (RFQ-EPR), and rapid freeze-quench Mössbauer (RFQ-Möss) spectroscopies, the three complementary methods which were used to delineate the kinetics of the excess Fe^{2+} reaction.[7] Thus, the results provide the basis for the experiments of the present study, in which these methods have been used to probe the kinetically and spectroscopically more complex reaction of apo R2 with limiting Fe^{2+} (Fe^{2+}/R2 = 2.0–2.4).

In our previous work[2] we showed that development of the optical and EPR spectra of the R2 cofactor differs markedly in the limiting Fe^{2+} reaction from that observed in the excess Fe^{2+} reaction. Perhaps the most striking difference is the rapid development in the limiting Fe^{2+} reaction of a broad, transient absorption band centered near 560 nm. Decay of this feature occurs concomitantly with formation of •Y122, which was interpreted as evidence that the absorbing species generates •Y122. On the basis of excellent chemical precedent[8] and the similarity of the observed absorption feature to that of an inorganic model complex,[9] the transient chromophore was tentatively proposed to be a μ-peroxodiferric cluster.[10] The one-electron oxidation of Y122 by this cluster was

* Authors to whom correspondence should be addressed.
§ Massachusetts Institute of Technology.
† Department of Physics, Emory University.
‡ Department of Biochemistry, Emory University.
⊥ Present address: Department of Biological Chemistry and Molecular Pharmacology, Harvard Medical School, Boston, MA 02115.
∥ Present address: Department of Chemistry, Carnegie Mellon University, Pittsburgh, PA 15213.
⊕ Abstract published in *Advance ACS Abstracts*, August 15, 1994.

(1) Atkin, C. L.; Thelander, L.; Reichard, P.; Lang, G. *J. Biol. Chem.* **1973**, *248*, 7464–7472.
(2) Bollinger, J. M., Jr.; Edmondson, D. E.; Huynh, B. H.; Filley, J.; Norton, J. R.; Stubbe, J. *Science* **1991**, *253*, 292–298.
(3) Bollinger, J. M., Jr.; Stubbe, J.; Huynh, B. H.; Edmondson, D. E. *J. Am. Chem. Soc.* **1991**, *113*, 6289–6291.
(4) Part 1: Ravi, N.; Bollinger, J. M., Jr.; Huynh, B. H.; Edmondson, D. E.; Stubbe, J. *J. Am. Chem. Soc.*, first of three papers in this issue.
(5) Ochiai, E.-I.; Mann, G. J.; Gräslund, A.; Thelander, L. *J. Biol. Chem.* **1990**, *265*, 15758–15761.
(6) Elgren, T. E.; Lynch, J. B.; Juarez-Garcia, C.; Münck, E.; Sjöberg, B.-M.; Que, L., Jr. *J. Biol. Chem.* **1991**, *266*, 19265–19268.
(7) Part 2: Bollinger, J. M., Jr.; Tong, W. H.; Ravi, N.; Huynh, B. H.; Edmondson, D. E.; Stubbe, J. *J. Am. Chem. Soc.*, second of three papers in this issue.
(8) Brennan, B. A.; Chen, Q.; Juarez-Garcia, C.; True, A. E.; O'Connor, C. J.; Que, L., Jr. *Inorg. Chem.* **1991**, *30*, 1937–1943 and references cited therein.
(9) Menage, S.; Brennan, B. A.; Juarez-Garcia, C.; Münck, E.; Lawrence Que, L., Jr. *J. Am. Chem. Soc.* **1990**, *112*, 6423–6425.
(10) The 560 nm absorbing species was proposed in ref 2 to be a μ-peroxodiferric cluster and was therein designated ***U***. For reasons which will become apparent, the absorbing species will no longer be referred to as ***U***. In general, we have amended our nomenclature such that the postulated intermediate states of R2 are now designated as **I**, **II**, and **II′** (see Scheme 1 in paper 1 of this series[4]). The diferric radical species, which is shown in Scheme 1 as a component of **II′**, is still designated as ***X***.

0002-7863/94/1516-8024$04.50/0

Scheme 1. Mechanism Previously Proposed To Be the Predominant Pathway in the Reaction of Apo R2 with Limiting Fe^{2+} (Reference 2)[a]

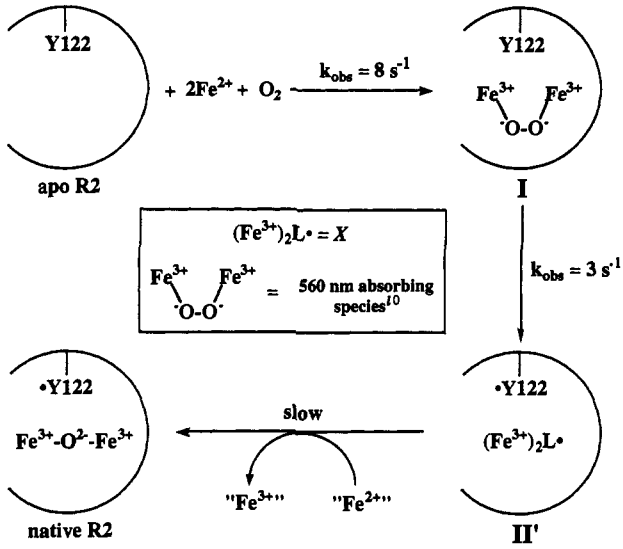

[a] The broken circles represent one monomer of the R2 dimer.

proposed to simultaneously generate •Y122 and ***X*** (Scheme 1).[10] The slowest step in the reaction was proposed to be reduction of ***X*** by Fe^{2+} to yield the product cofactor.[2]

In the experiments which are described in this paper, RFQ-Mössbauer was used in an attempt to obtain direct evidence for the postulated μ-peroxodiferric cluster of **I** and to further test the mechanism of Scheme 1. The Mössbauer kinetic data, when compared with optical and EPR data acquired under identical reaction conditions, are largely consistent with this mechanism. The data indicate, however, that the only iron-containing component of **I** is, in fact, ***X***. This result implies that our previous assignment of the 560 nm absorbing species of **I** as a μ-peroxodiferric cluster is incorrect. On the basis of this result, additional spectroscopic evidence, chemical precedent from the pulse radiolysis literature,[11] and biochemical precedent from yeast cytochrome *c* peroxidase,[12] we propose herein that **I** contains a tryptophan radical cation (•WH^+), which is responsible for the 560 nm absorption band and which generates •Y122 in the rapid phase of the reaction. We further speculate as to the identity of the W residue which is oxidized and discuss the implications of our revised hypothesis with respect to the catalytic mechanisms of RNR and other dinuclear iron proteins. Finally, we elaborate on our hypotheses (1) that **I** also forms in the excess Fe^{2+} reaction, but does not accumulate to detectable levels, and (2) that the fate of **I** (and therefore which pathway the reaction follows) is determined by the availability of the extra electron.

Materials and Methods

Materials. Apo R2 and apo R2-Y122F were prepared as described in the supplementary material to paper 2 of this series.[7] Protein concentrations were determined from absorbance at 280 nm by using the published molar absorption coefficient of 120 mM^{-1} cm^{-1}.[13] Natural abundance (^{56}Fe) iron wire was purchased from Baker (Phillipsburg, NJ). ^{57}Fe metal (>95% enrichment) was purchased from Advanced Materials and Technology (New York, NY). 2-Methylbutane was purchased from Aldrich (Milwaukee, WI). Ferrozine and the Fe atomic absorption standard were purchased from Sigma (St. Louis, MO).

Time-Course of the Reaction of Apo R2 with O_2 and Limiting Fe^{2+} Monitored by SF-Abs, RFQ-EPR, and RFQ-Mössbauer. In all of the RFQ-EPR and RFQ-Mössbauer experiments and in most of the SF-Abs experiments, 0.59–0.62 mM apo R2 (or apo R2-Y122F) in O_2-saturated 100 mM HEPES (pH 7.7) was mixed at 5 °C with an equal volume of O_2-saturated $^{56}Fe^{2+}$ or $^{57}Fe^{2+}$ stock solution in 2–3 mM H_2SO_4. The concentration of Fe^{2+} in the stock was such that the Fe^{2+}/R2 ratio was 2.2–2.4. Preparation of the Fe^{2+} stock and saturation of both stock solutions with O_2 is described in the preceding paper.[7] With the exception of the difference in Fe^{2+}/R2, the kinetic experiments and analyses were carried out as described in the preceding paper.[7] RFQ-Mössbauer samples were prepared as described in paper 1 of this series.[4]

In other SF-Abs experiments, lower concentrations of apo R2 were employed. In these cases, an air-saturated Fe^{2+} solution was mixed at 5 °C with an equal volume of air-saturated apo R2 solution in 100 mM HEPES (pH 7.7). The Fe^{2+} stock solutions were prepared by dissolution of $FeSO_4 \cdot 7H_2O$ in 5 mM HNO_3, HCl, or H_2SO_4. The reactant concentrations used in each experiment are listed in the appropriate figure legend.

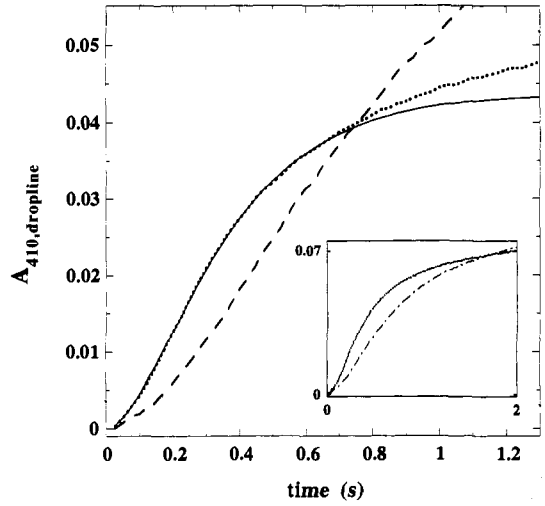

Figure 1. Kinetics of •Y122 production (as assessed by $A_{410,dropline}$) in the reconstitution of R2 with limiting Fe^{2+} (dotted traces of main figure and inset), excess Fe^{2+} (dashed trace), or limiting Fe^{2+} and ascorbate (dot-dashed trace of inset). The solid trace is a fit of eq 1 to 0.005–0.7 s of the limiting Fe^{2+} trace. It corresponds to $k_1 = 6.7\ s^{-1}$, $k_2 = 4.5\ s^{-1}$, and $[•Y122]_\infty \epsilon_{410,dropline} = 0.044$. The experimental traces of the main figure were constructed as $A_{410} - (3A_{406} + 2A_{416})/5$ from the averages of four trials for each wavelength. The reaction conditions were the following: 5 ± 0.5 °C, 50 mM HEPES (O_2-saturated), pH 7.6, 0.295 mM apo R2, and either 0.67 mM Fe^{2+} (limiting Fe^{2+}, dotted trace) or 1.45 mM Fe^{2+} (excess Fe^{2+}, dashed trace). The traces of the inset were constructed as $A_{410} - (A_{404} + A_{416})/2$ from the averages of three trials for each wavelength. The reaction conditions were the following: 5 ± 0.5 °C, 50 mM HEPES (air-saturated), pH 7.6, 54 μM apo R2, and either 124 μM Fe^{2+} (dotted trace) or 126 μM Fe^{2+} and 2.5 mM ascorbate (dot-dashed trace).

Results

Time-Course of the Limiting Fe^{2+} Reaction by SF-Abs. As previously reported,[2] development of the absorption spectrum of the R2 cofactor differs markedly in the reaction of apo R2 with limiting Fe^{2+} (2.0–2.4 molar equiv) from that observed in the excess Fe^{2+} reaction.[7] The limiting Fe^{2+} reaction requires 60–120 s to reach completion, compared to less than 30 s for the excess Fe^{2+} reaction. In spite of this fact, and in spite of the fact that the final quantity of •Y122 produced is greater in the excess Fe^{2+} reaction, $A_{410,dropline}$-versus-time traces[7] for the reactions indicate that formation of •Y122 is initially *faster* and has a considerably *shorter* lag time in the *limiting* Fe^{2+} reaction (Figure 1, dotted trace) than in the excess Fe^{2+} reaction (Figure 1, dashed trace). This unexpected trend holds throughout the greater than 10-fold range of [R2] (22–290 μM) which was investigated. The relatively fast phase of •Y122 production is not observed when ascorbate is included in the limiting Fe^{2+} reaction (inset of Figure 1), again despite the fact that more •Y122 is produced when ascorbate is included. At completion of the limiting Fe^{2+} reaction,

(11) Solar, S.; Getoff, N.; Surdhar, P. S.; Armstrong, D. A.; Singh, A. *J. Phys. Chem.* **1991**, *95*, 3639–3643 and references cited therein.
(12) Houseman, A. L. P.; Doan, P. E.; Goodin, D. B.; Hoffman, B. M. *Biochemistry* **1993**, *32*, 4430–4443 and references cited therein.
(13) Thelander, L. *J. Biol. Chem.* **1973**, *248*, 4591–4601.

Scheme 2. Kinetic Scheme Used in Analysis of SF-Abs Data[a]

$$\mathbf{A} \xrightarrow{k_1} \mathbf{I}\ (560\ \text{nm abs.}) \xrightarrow{k_2} \mathbf{II}'(\cdot\text{Y122})$$

[a] A represents the three reactants.

Table 1. Summary of Least-Squares Fits of Eq 1 to $A_{410,\text{dropline}}$-versus-Time Traces from the Reaction of Apo R2-wt with Limiting Fe^{2+}

expt[a]	fit range (s)	k_1 (s^{-1})	k_2 (s^{-1})	A_{fit}/A_{total}[b]
1[c]	0.010–0.700	5.1	5.0	0.66
2[d]	0.025–0.400	5.6	5.0	0.63
	0.025–0.600	5.5–6.7[e]	4.4–5.4[e]	0.61–0.62[e]
	0.025–0.800	5.6–8.0[e]	3.6–5.0[e]	0.62–0.64[e]
	0.025–1.00	9.7	3.0	0.67
	0.025–1.20	11.2	2.7	0.69
	0.025–1.60	13.9	2.3	0.72

[a] The conditions employed in experiments 1 and 2 are listed in the legend to Figure 1 (Experiment 1 corresponds to the main figure and experiment 2 to the inset). [b] The amplitude for $A_{410,\text{dropline}}$ given in the fit compared to the total amplitude at completion. [c] 4–6 trials averaged at each wavelength. [d] 3–4 trials averaged at each wavelength. [e] Varied within this range depending on the initial estimates for k_1 and k_2.

the magnitude of $A_{410,\text{dropline}}$ implies an Fe^{2+}/•Y122 stoichiometry of 3.0 ± 0.2. This stoichiometry, which is independent of [R2] within the range examined, is consistent with the conclusion that Fe^{2+} supplies the extra electron which is required for electron balance.[5-7]

Figure 1 illustrates that •Y122 formation in the limiting Fe^{2+} reaction is multiphasic, in contrast to the biphasic kinetics of the excess Fe^{2+} reaction.[7] This kinetic complexity is expected, for two reasons. First, the Fe^{2+}/R2 ratio employed (2.0–2.4) is insufficient to saturate the Fe-binding sites. Results obtained with Fe^{2+}/R2 ratios of ~1 demonstrate that the reaction is markedly slowed (requiring in excess of 2 min to reach completion) as a consequence of Fe^{2+} being sub-saturating.[14] This slowing has been attributed to the rate-limiting rearrangement of unreactive mononuclear ferrous–R2 complexes[15] into the reactive diferrous form.[14] Second, Fe^{2+}/R2 is probably not sufficiently *low* to prevent a contribution from the excess Fe^{2+} reaction pathway.[7] Thus, several kinetic phases are expected.

Consistent with the proposed mechanism (Scheme 1), the lag phase in the limiting Fe^{2+} trace of Figure 1 indicates that an intermediate accumulates prior to •Y122 production. In order to estimate rate constants for formation of the inferred intermediate and for the fast phase of •Y122 production, the early portions (0–0.8 s) of $A_{410,\text{dropline}}$-versus-time traces were analyzed according to eq 1, which is appropriate for the kinetic mechanism of Scheme 2. In this scheme, all steps in the reaction are assumed to be irreversible. Values of 5–8 s^{-1} for k_1 and 3.6–5.4 s^{-1} for k_2 were obtained (Table 1). The fit shown in Figure 1 (solid line) corresponds to k_1 = 6.7 s^{-1} and k_2 = 4.5 s^{-1}. The amplitude associated with k_2 in this fit corresponds to 60% of the total amplitude of $A_{410,\text{dropline}}$ in this experiment. This result, which is representative of those obtained in several experiments with similar Fe^{2+}/R^2 ratios (Table 1), suggests that ~$^2/_3$ of the •Y122 produced in the reaction is generated in the rapid initial phase.

(14) Bollinger, J. M., Jr. Ph.D. Thesis, Massachusetts Institute of Technology, 1993.

(15) On the basis of efficient reconstitution of R2 by even sub-stoichiometric quantities of added Fe^{2+}, it has been suggested that the individual binding sites for the dinuclear cluster are highly cooperative (i.e. that binding of Fe^{2+} to the apo protein results exclusively in diferrous–R2 complexes).[6,38,39] Such cooperativity has not been demonstrated, and it has been shown that the above interpretation is incorrect.[14] While our experiments do not address the issue of thermodynamic cooperativity between the Fe sites, they do suggest that the kinetic preference for dinuclear binding over mononuclear binding is, at most, slight.

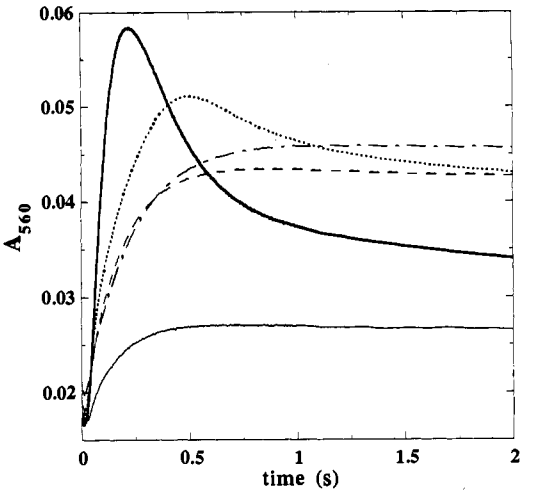

Figure 2. SF-Abs titration to determine the Fe^{2+}/R2 ratio required to suppress the 560 nm transient. Reaction conditions were the following: 5 ± 0.5 °C, 50 mM HEPES (air-saturated), pH 7.6, 54 μM apo R2, and either 124 μM Fe^{2+} (thick solid trace), 217 μM Fe^{2+} (dotted trace), 270 μM Fe^{2+} (dashed trace), 504 μM Fe^{2+} (dot-dashed trace), or 126 μM Fe^{2+} and 2.5 mM sodium ascorbate (thin solid trace). Each trace represents the average of 3–4 trials. The limiting Fe^{2+} and limiting Fe^{2+} + ascorbate traces converge at increased reaction times (~30 s).

$$A_{410,\text{dropline}}(t) = [\cdot\text{Y122}]_\infty \epsilon_{410,\text{dropline}} \times \left(1 + \frac{k_1 \exp(-k_2 t) - k_2 \exp(-k_1 t)}{k_2 - k_1}\right) \quad (1)$$

As reported in our previous work,[2] the most striking SF-Abs evidence for the accumulation of an intermediate in the limiting Fe^{2+} reaction is provided by a broad, transient absorption band centered at 560 nm (Figure 2, thick solid trace). In several experiments, the time of maximum absorbance at 560 nm (t_{max}) was observed to vary between 0.18 and 0.25 s (Table 2). Also as previously reported, the transient is not observed in the excess Fe^{2+} reaction: its development is completely suppressed by an Fe^{2+}/R2 ratio of 5 (Figure 2, dashed trace) (but not completely by a ratio of 4, dotted trace). The transient also is not observed when the reaction is carried out with limiting Fe^{2+} and ascorbate (Figure 2, thin solid trace). In addition to illustrating the extreme sensitivity of the reaction kinetics to changes in the Fe^{2+}/R2 ratio and/or to the presence of additional reductants, the data of Figures 1 and 2 illustrate the correlation between accumulation of the 560 nm absorbing species and the presence of a relatively fast phase of •Y122 production. This correlation strongly suggests that the 560 nm absorbing species generates •Y122 in the fast phase of the limiting Fe^{2+} reaction.

In an attempt to estimate rate constants for formation and decay of this species and its molar absorptivity at 560 nm (ϵ_{560}), non-linear least-squares analysis of A_{560}-versus-time traces was carried out. The 0–3 s regions of several traces were analyzed according to eq 2,which gives absorbance as a function of time

$$A_t = A_\infty + \alpha \exp(-k_1 t) + (A_0 - A_\infty - \alpha) \exp(-k_2 t) \quad (2)$$

(A_t) for a reaction involving two consecutive, first-order processes (Scheme 2). (It should be noted that our mechanistic hypothesis involves three consecutive processes, of which only one (conversion of **I** to **II**′) would necessarily be first order under these reaction conditions. Fitting according to a three-step model is feasible, but it would be uninformative due to the excessive number of parameters required. Furthermore, conversion of **II**′ to native R2 should cause minimal change in the absorbance at 560 nm, since ***X*** absorbs weakly at this wavelength. Thus, Scheme 2 is adequate to provide estimates for the rate constants of the first two steps.) In eq 2, A_0 is the absorbance at t = 0, A_∞ is the

Table 2. Summary of Selected Least-Squares Fits to Eq 2 of A_{560}-versus-Time Traces from the Reaction of Apo R2-wt with Limiting Fe^{2+}

exp[a]	t_{max}(s)	fit range (s)	A_0	k_1 (s^{-1})[b]	k_2 (s^{-1})[b]	ϵ_{560}[c] (M^{-1} cm^{-1})
1[d]	0.220	0.005–3.00	fixed	5.5	4.4	1900
		0.005–3.00	fixed	3.8	6.2	2800
		0.005–0.945	fixed	6.6	3.4	1700
		0.055–1.10	varied	7.2	6.7	1500
2[d]	0.185	0.005–2.50	fixed	6.7	5.5	2000
		0.005–2.50	fixed	5.4	6.9	2300
		0.035–0.695	varied	9.7	6.6	2900

[a] Reaction conditions were identical with those in the corresponding experiments of Table 1. [b] The assignment of one k_{obs} as k_1 and the other as k_2 is arbitrary, since the relative magnitudes of k_1 and k_2 depend on the initial estimate for α. [c] Calculated according to eq 5, as described in the text. [d] A_{560} versus time trace analyzed represents the average of 3 trials.

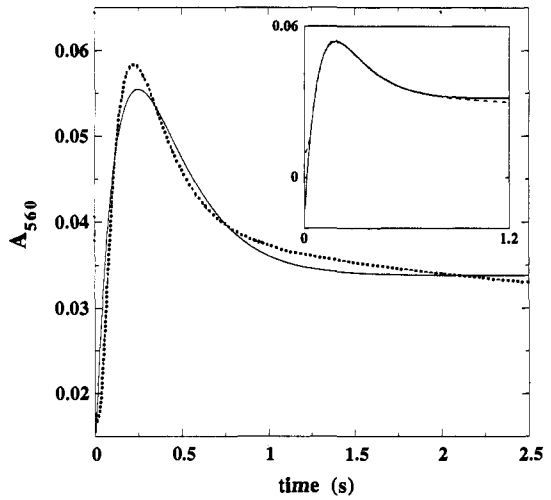

Figure 3. Non-linear least-squares analysis of A_{560}-versus-time traces from the limiting Fe^{2+} reaction. The dotted trace in the main figure is the limiting Fe^{2+} trace from Figure 2. The solid trace is a fit of eq 2 (with A_0 fixed) to the data. It corresponds to k_1 = 6.0 s^{-1} and k_2 = 4.0 s^{-1}. The dashed trace in the inset was acquired under the reaction conditions listed for Figure 1. It represents the average of four trials. The solid trace is a fit (with A_0 allowed to vary), corresponding to k_1 = 9.7 s^{-1} and k_2 = 6.6 s^{-1}.

absorbance at $t = \infty$, and α is related to the molar absorptivities of species A, I, and II′ (ϵ_A, ϵ_I, and $\epsilon_{II'}$, respectively), the rate constants k_1 and k_2, and the concentration of species A at $t = 0$ ($[A]_0$), by eq 3.[16] Fits were generated either with A_0 fixed to the

$$\alpha = \frac{[(\epsilon_I - \epsilon_A)k_1 + (\epsilon_A - \epsilon_{II'})k_2]}{(k_2 - k_1)}[A]_0 \qquad (3)$$

experimental initial absorbance or with A_0 allowed to vary. With A_0 fixed (Figure 3, solid trace), the analysis gave values of 5.3–8.8 s^{-1} for one rate constant and values of 3.4–5.5 s^{-1} for the second rate constant (Table 2). Due to the existence of dual solutions in consecutive reactions,[16] and because the value of ϵ_I is not known, it is not possible to deduce *a priori* which rate constant corresponds to formation of the 560 nm absorbing intermediate and which corresponds to its decay. Nevertheless, the values for the larger k_{obs} correspond well with the range of 5–8 s^{-1} calculated for k_1 by fitting the $A_{410,dropline}$-versus-time curves (Table 1). Likewise, the range for the smaller k_{obs} agrees well with the range of 3.6–5.4 s^{-1} calculated for k_2 by fitting the $A_{410,dropline}$-versus-time curves. Therefore, the kinetics of development and decay of the 560 transient and of formation of •Y122 are consistent with the proposal that the transient species generates •Y122 in the fast phase of the reaction.

The A_{560nm}-versus-time traces are poorly fit according to the oversimplified kinetic model of Scheme 1 when the value of A_0 is held fixed (Figure 3, solid trace). In the rise phase of the transient, the experimental trace lags behind the theoretical trace. This observation suggests that there is a lag phase in formation of the 560 nm absorbing intermediate, which suggests that some intermediate accumulates prior to the absorbing species. In the region of t_{max}, the theoretical curve does not rise and fall as sharply as the experimental trace, and it fails to reach as great a maximum absorbance as the experimental trace. These observations suggest that the values of k_1 and k_2 obtained in the fit may be underestimates of the true values. The shape of the experimental trace in the region of t_{max} can be more accurately reproduced if the lag phase is excluded from the fit-range and if the value of A_0 is allowed to vary in the fit. Fitting to the experimental traces in this manner (inset of Figure 3, solid trace) gave maximum values for the two rate constants of 9.7 and 6.6 s^{-1}, indicating that fitting with A_0 fixed at most only slightly underestimates the rate constants.

From the parameters obtained in fitting the A_{560nm}-versus-time curves, the molar absorptivity at 560 nm of intermediate I (ϵ_I in eq 3) was estimated. Solving eq 3 for ϵ_I gives eq 4. In

$$\epsilon_I = \frac{\alpha(k_2 - k_1) - [A]_0(\epsilon_A - \epsilon_{II'})k_2}{[A]_0 k_1} + \epsilon_A \qquad (4)$$

modeling the reaction by Scheme 2, species A corresponds either to an Fe(II)–R2 complex or to Fe^{2+} and apo R2 in solution. Neither of these species absorbs at 560 nm, so ϵ_A of eq 4 can be set to zero. (Since species A does not absorb, the non-zero value of A_0 is merely an offset to account for the small amount of light scattering by the protein.) Equation 4 thus reduces to eq 5. $[A]_0\epsilon_{II'}$

$$\epsilon_I = \frac{\alpha(k_2 - k_1) + [A]_0\epsilon_{II'}k_2}{[A]_0 k_1} \qquad (5)$$

is simply the value of $A_\infty - A_0$ from the fit. $[A]_0$ can be estimated as the concentration of •Y122 at completion, which is one-third the Fe^{2+} concentration after mixing. With these assumptions, the values calculated for ϵ_I from all the fits described above ranged from 1500 to 2900 M^{-1} cm^{-1} (Table 2). However, the above analysis of the $A_{410,dropline}$-versus-time traces suggests that only ~60% of the •Y122 generated in the reaction is produced in the fast phase (Table 1). This result suggests that the final concentration of •Y122 is an overestimate of $[A]_0$ by a factor of 1/0.6. The range calculated for ϵ_I with $[A]_0$ corrected by this factor would be 2500–4800 M^{-1} cm^{-1}.

Time-Course of the Limiting Fe^{2+} Reaction of R2-Y122F by SF-Abs. As with the wild-type protein (R2-wt), when apo R2-Y122F is mixed at 5 °C with limiting Fe^{2+}, a broad absorption band centered at 560 nm rapidly develops.[2] This result indicates that residue Y122 is not required for formation of the 560 nm absorbing species. Also as in R2-wt, the transient is not seen in the reaction of apo R2-Y122F with excess Fe^{2+} nor with limiting Fe^{2+} and ascorbate. In the mutant protein, t_{max} at 560 nm is 300–400 ms (the range observed in five experiments), which is significantly greater than in R2-wt. This result suggests that formation or decay (or both) of the 560 nm absorbing species is slower in R2-Y122F than in R2-wt. Fitting eq 2 (with A_0 fixed) to A_{560}-versus-time traces gave values of 2.8–3.2 s^{-1} for one rate constant and values of 2.3–2.7 s^{-1} for the second rate constant. Calculating ϵ_I from these fits according to eq 5 gave values of 1700–2800 M^{-1} cm^{-1}, in excellent agreement with the range calculated above from the apo R2-wt limiting Fe^{2+} reaction. These results suggest that formation and decay of the intermediate are both slower in R2-Y122F than in R2-wt. As previously argued,[2]

(16) Espenson, J. H. *Chemical Kinetics and Reaction Mechanisms*; McGraw-Hill: New York, 1981.

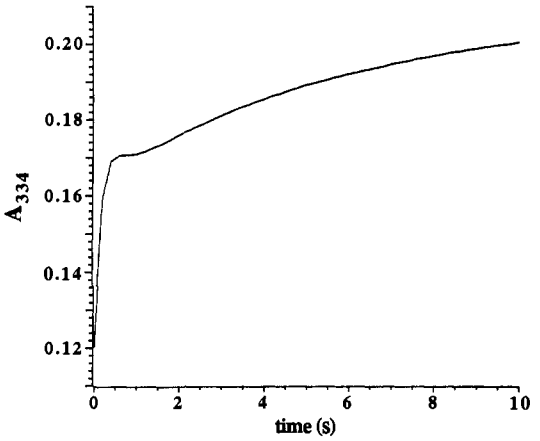

Figure 4. SF-Abs evidence for a ~335 nm absorption band associated with the 560 nm absorbing species in the reaction of apo R2-Y122F with limiting Fe^{2+}. The reaction conditions were the following: 24 μM apo R2-Y122F, 53 μM Fe^{2+}, 50 mM HEPES (air-saturated), pH 7.6, 5 ± 0.5 °C. The data were acquired on the previously described Applied Photophysics RX1000/Hewlett Packard HP8452A apparatus.[2] The trace represents the average of three trials.

the increased lifetime of the intermediate in the mutant protein is additional evidence that it generates •Y122 in the reaction of apo R2-wt with limiting Fe^{2+}.

In addition to the obvious features discussed above (560 nm) and in our previous work (325 and 365 nm features of the diferric cluster, 360 nm feature of ***X***, and transient, sharp band at 410 nm tentatively assigned to an unstable tyrosyl radical[2]), the early spectra of the R2-Y122F limiting Fe^{2+} reaction appear to exhibit a broad band near 335 nm. The A_{334}-versus-time trace (Figure 4) provides support for this assertion. The trace exhibits at least three phases. The first two are characterized by a rapid increase (from 0 to ~0.6 s), followed by a plateau (from ~0.6 to 1.2 s) or, in some experiments, a slight decrease. Subsequent to this plateau (or decay) phase, the curve rises monotonically. The complexity of this trace precludes meaningful fitting, but it appears that the rapid rise phase corresponds temporally with the formation of the 560 nm absorbing species, and that the plateau (or decay) phase corresponds with decay of the 560 nm transient. In addition, re-examination of the time-dependent spectra of the reaction of apo R2-wt with limiting Fe^{2+} [2] suggests that the 335 nm band develops in this reaction as well. These results suggest that the band near 335 nm may be associated with the 560 nm absorbing species. As discussed below, the apparent association of these features provides a valuable clue as to the identity of the species.

Time-Course of the Limiting Fe^{2+} Reaction by RFQ-Möss. The SF-Abs data strongly suggest that the 560 nm absorbing species is responsible for the rapid phase of •Y122 production in the limiting Fe^{2+} reaction. As noted above, we previously proposed that this species is a μ-peroxodiferric cluster. In the present study, evidence for such a cluster was sought by using RFQ-Möss. As in our study of the excess Fe^{2+} reaction,[7] a complete time-course of the limiting Fe^{2+} reaction was carried out. The time-dependent spectra clearly reflect the progress of the reaction. At a reaction time of 0.061 s (Figure 5A), the features of unreacted ferrous ion dominate the spectrum, but a significantly quantity of ***X*** has already formed. The spectrum of the diferric cluster is not yet apparent. At somewhat longer reaction times (0.28 s, Figure 5B), the contribution to the spectrum from ferrous ion has decreased, while the contribution due to ***X*** has increased. In addition, the features of the diferric cluster are now visible. Finally, near completion of the reaction (60 s, Figure 5D), the features of the diferric cluster dominate the spectrum.

Parts A and B of Figure 5 illustrate that the features which would be expected for the proposed μ-peroxodiferric species are absent from the early spectra of the reaction. The model complex

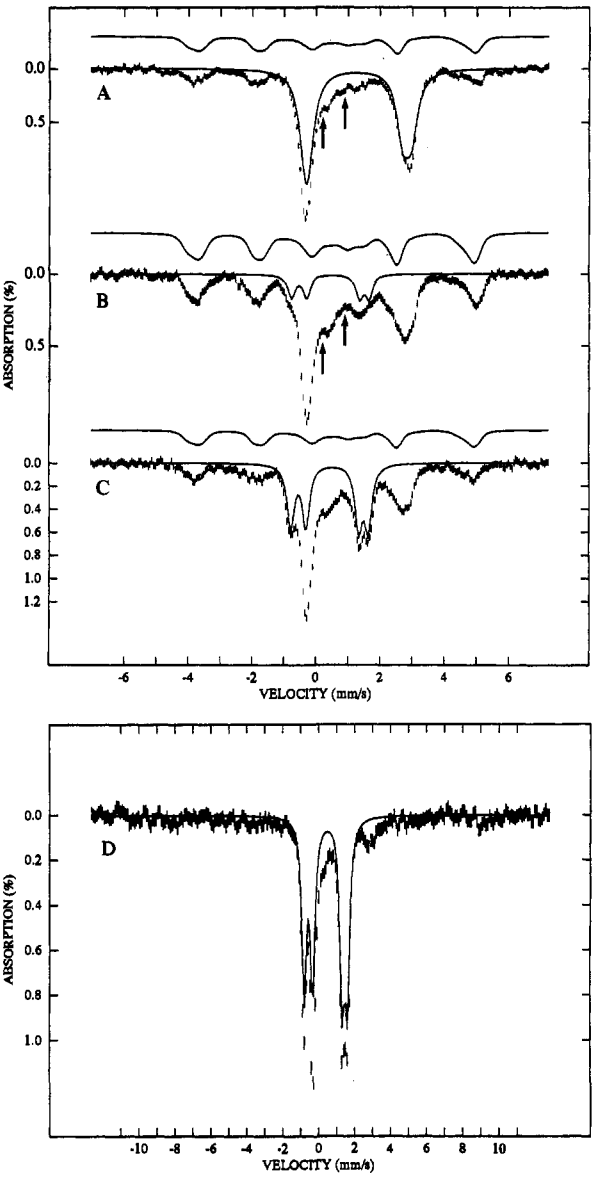

Figure 5. Time-course of the reaction of apo R2 with limiting Fe^{2+} monitored by RFQ-Möss. The spectra are of samples from experiment 1 of Table III (supplementary material). The reaction conditions were the following: 0.30 mM apo R2, 0.67 mM Fe^{2+}, 5 ± 1 °C, 50 mM HEPES (O_2-saturated), pH 7.6. The reaction was quenched (A) at 0.061, (B) 0.28, (C) 1.0, or (D) 60 s. The solid line plotted over the data in part A is the theoretical reference spectrum of ferrous–R2 (see preceding paper[7]) scaled to 55% of the integrated intensity of the experimental spectrum. The spectrum just above the data in parts A–C is the theoretical reference spectrum of ***X*** (25% in A, 45% in B, and 25% in C). The solid line plotted over the data in parts B–D is the theoretical reference spectrum of the diferric cluster (13% in B, 35% in C, 60% in D). The experimental spectra were acquired at 4.2 K with a magnetic field of 50 mT applied parallel to the γ-beam.

of Que and co-workers, on which our tentative structural assignment was partly based, exhibits a single quadrupole doublet (ΔE_Q = 0.72) with isomer shifts (δ = 0.52) characteristic of high-spin ferric ions.[9] The arrows in parts A and B of Figure 5 indicate the positions of these features. If the 560 nm absorbing species were, in fact, a μ-peroxodiferric cluster and it exhibited one or two quadrupole doublets with isomer shifts similar to those of the model complex, the features should easily have been detected in these spectra. The absence of such features suggests that the 560 nm absorbing species is not a μ-peroxodifferic cluster. Moreover, no features whatsoever are apparent which develop and decay in temporal correlation with the 560 nm absorption

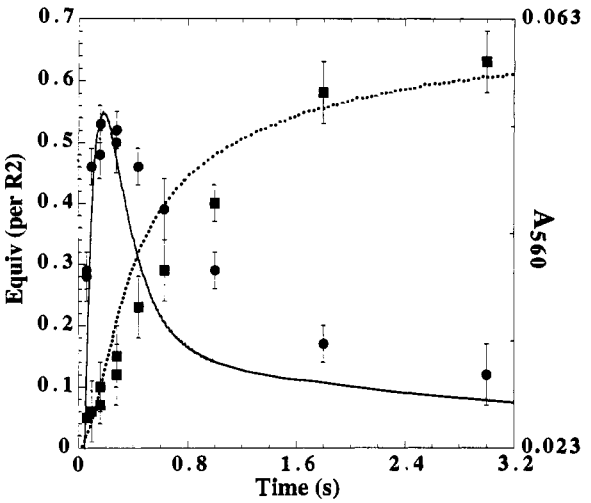

Figure 6. A_{560} (solid trace) and quantities of ***X*** (circles), diferric cluster (squares), and •Y122 (dotted trace) as functions of time for the reaction of apo R2 with limiting Fe^{2+}. The reaction conditions were as in Figure 5. Note: The right-hand access applies only to A_{560} and is scaled as described in the text for purposes of comparison.

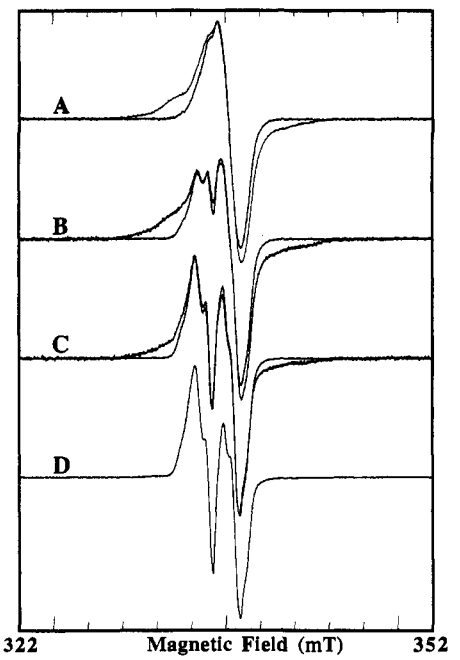

Figure 7. Time-course of the reaction of apo R2-wt with limiting Fe^{2+} monitored by RFQ-EPR. Reaction conditions were as in Figure 5. The reaction was quenched (A) at 0.15, (B) 0.44, (C) 1.0, or (D) 60 s. The outer lines are the experimental spectra. They were acquired at 20 K with a microwave power of 2 μW. Other spectrometer settings are listed in the preceding paper.[7] The inner lines in parts A–C, which are intended to illustrate the presence of broad features in the outer spectra, are summations of the spectra of ***X*** and •Y122 in ratios (***X***:•Y122 = 83:17 in A, 56:44 in B, and 22:78 in C) appropriate to reproduce the line shapes of the outer spectra.[7]

transient. This observation suggests that the 560 nm absorbing species does not contain iron.

As in the excess Fe^{2+} reaction, the time-dependent spectra of the limiting Fe^{2+} reaction allow both ***X*** and the diferric cluster to be quantified as functions of reaction time (Figure 6). The quantity of ***X*** present in the reaction (circles) increases rapidly without a significant lag phase, reaches its maximum value (~0.55 equiv) at some time between 0.15 and 0.28 s, and then decreases slowly. After an apparent lag phase, the quantity of diferric cluster (squares) increases smoothly.

Comparison of RFQ-Mössand SF-Abs Data. For comparison with the RFQ-Möss data, the time-courses for formation of •Y122 (as determined by $A_{410,\text{dropline}}$, dotted trace) and for development and decay of the 560 nm absorption band (solid trace) are also shown in Figure 6. These data are from a SF-Abs experiment with identical reaction conditions. The A_{560}-versus-time trace is scaled so that the final absorbance coincides with zero on the left-hand axis and so that the maximum value of the trace coincides with the maximum quantity of ***X***. It is apparent that the t_{max} of ***X*** and that of A_{560} (0.19 s in this experiment) roughly coincide and that decay of ***X*** is significantly slower than decay of the absorption transient. These data imply that ***X*** accumulates concomitantly with the development of the 560 nm absorption band characteristic of intermediate **I**. This result indicates that ***X*** is a component of **I**, for if ***X*** were a component only of **II′**, its formation would exhibit a lag phase and would be slower than development of the 560 nm absorption band. ***X*** is not, however, the 560 nm absorbing component of **I**, as the 560 nm band is not observed in the excess Fe^{2+} reaction (Figure 2), even though ***X*** accumulates to 1 equiv.[7] Thus, **I** must consist of ***X*** and a second species, which does not contain iron and which is responsible for the 560 nm absorption. The fact that decay of the 560 nm transient is faster than decay of ***X*** suggests that ***X*** is also a component of **II′**, the intermediate which results from decay of **I**.

Examination of Figure 6 also reveals that formation of •Y122 is initially faster than formation of the diferric cluster, as would be predicted from Scheme 1. Mössbauer quantitation on the 0.63 s sample indicates that 0.29 ± 0.04 equiv of the diferric cluster is present, while stopped-flow experiments carried out under identical reaction conditions indicate that 0.39 ± 0.03 equiv of •Y122 is present at this same time. Three considerations provide support for the conclusion that formation of •Y122 is faster than formation of the diferric cluster. First, the maximum difference between the curves (0.1 equiv at ~0.6 s) is greater than the sum of the uncertainties which we estimate for the values. Second, the measured quantity of •Y122 is greater than the measured quantity of diferric cluster over a time-range that spans five Mössbauer samples. Third, the rate constants measured for the excess Fe^{2+} reaction by RFQ-Möss are marginally greater than those measured by SF-Abs.[7] Thus, the amount by which the quantity of •Y122 exceeds the quantity of diferric cluster at a given reaction time might actually be greater. The observation that •Y122 forms faster than the diferric cluster is consistent with the proposed accumulation of the intermediate **II′**, which contains •Y122 but not the diferric cluster.

Time-Course of the Limiting Fe^{2+} Reaction by RFQ-EPR. In our mechanism for the limiting Fe^{2+} reaction (Scheme 1), both components of the intermediate **II′** (***X*** and •Y122) are known to be EPR active. Therefore, for comparison with the SF-Abs and RFQ-Möss data, the time-course of the limiting Fe^{2+} reaction was monitored by RFQ-EPR (Figure 7). The spectrum at short times (Figure 7A, outer line) resembles the isotropic singlet characteristic of ***X***. The spectra at increasingly longer reaction times show an increasing contribution from •Y122 and a decreasing contribution from ***X*** (Figure 7, parts B and C, outer lines). In addition to the features of ***X*** and •Y122, broader features are readily apparent in Figure 7A–C. These broad features are observed at all reaction times from 0.061 to 3 s. In the early spectra, the broad features appear to contribute as much as (50 ± 10)% of the double-integrated intensity (as estimated by subtraction of the spectra due to •Y122 and ***X***, inner spectra of Figure 7A–C), indicating that the species that give(s) rise to these features accumulate(s) to concentrations which are comparable with those of **X** and •Y122. The features eventually decay to leave only the spectrum of •Y122 (Figure 7D). As argued in our previous work, one possible origin of the broad features is dipolar interaction between ***X*** and •Y122 in **II′**. The crystal structure of R2 reveals that Y122 is ~5 Å from one of

the ferric ions of the diferric cluster.[17,18] It is reasonable to expect, therefore, that *X* and •Y122 would be a comparably short distance apart in II′, close enough to experience mutual dipolar broadening.

Comparison of Mössand EPR Data. Possible support for the notion of dipolar broadening between *X* and •Y122 in II′ is provided by a quantitative comparison of the Mössbauer and EPR data. (Evidence from the preceding paper[7] suggests that quantitative comparisons can be made with confidence.) Comparison of the quantity of *X* measured for a given time-point by Mössbauer spectroscopy with the quantity of *X* recognizable in the EPR spectrum of the same time-point reveals an apparent inconsistency in the data. As an illustration of this point, consider the 1.0 s time-point. The Mössbauer spectrum of this sample indicates that 0.29 ± 0.03 equiv of *X* is present. The shape of the EPR spectrum of this time-point (Figure 7C) is best reproduced by an •Y122/*X* ratio between 72/28 and 78/22 (assuming that the spectra of •Y122 and *X* are unperturbed). This analysis would imply that 0.91 ± 0.18 equiv of •Y122/R2 is present at 1.0 s. This value is impossibly high: the stopped-flow data indicate that 0.5 ± 0.04 equiv of •Y122 is present at 1 s and that only 0.74 ± 0.03 equiv has formed after 60 s. Furthermore, at least 33% of the double-integrated intensity of the EPR spectrum is contributed by the broad features. This would imply that at least 1.5 equiv of total radical (*X* + •Y122 + species responsible for the broad features) is present at 1.0 s, a value which is also unreasonably high. Similar analyses of the 1.8 and 3 s spectra also give unreasonably large values for the quantities of •Y122 and total radical present. The Mössbauer and EPR spectra appear, therefore, to be discrepant in terms of the quantity of *X* which they reflect. The postulated simultaneous presence of *X* and •Y122 in II′, leading to dipolar broadening of the EPR spectra of both, provides a possible reconcilation of this apparent discrepancy.

Time-Course of the Limiting Fe^{2+} Reaction of R2-Y122F by RFQ-EPR. The broad EPR features in the reaction of apo R2-wt with limiting Fe^{2+} cannot arise solely from interaction of *X* and •Y122 in II′, however, as such features are also observed in the reaction of apo R2-Y122F with limiting Fe^{2+} (Figure 8A–C).[19] The development of the broad features in the limiting Fe^{2+} reaction of R2-Y122F, in which I can form but II′ cannot, suggests that the features may be associated with I, as well as with II′.

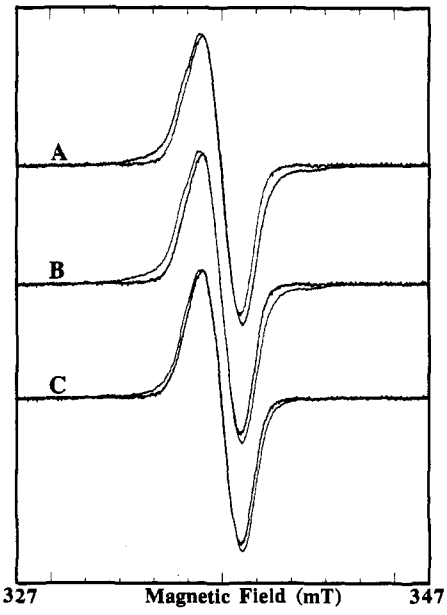

Figure 8. Time-course of the reaction of apo R2-Y122F with limiting Fe^{2+} monitored by RFQ-EPR. The reaction conditions were the following: 0.30 mM apo R2-Y122F, 0.65 mM Fe^{2+}, 5 ± 1 °C, 50 mM HEPES (O_2-saturated), pH 7.6. The reaction was quenched (A) at 0.15, (B) 0.44, or (C) 1.0 s. The outer line in each is the experimental spectrum, and the inner line is the spectrum of *X*.[7] The spectra were acquired as in Figure 7.

Discussion

As demonstrated in the preceding paper, the kinetics of the reaction of apo R2, O_2, and excess Fe^{2+} are consistent with the proposed three-component mechanism (Scheme 1 of the preceding paper[7]). Therefore, an argument for a different mechanism in the limiting Fe^{2+} reaction must first demonstrate that this additional complexity is required. The SF-Abs data provide the best evidence for a change of mechanism. •Y122 formation is initially faster in the limiting Fe^{2+} reaction than in the excess Fe^{2+} reaction. This unusual result is most reasonably accommodated by proposing that the reactions proceed by different mechanisms. Moreover, the observations that the presence of either excess Fe^{2+} or ascorbate prevents development of the 560 nm absorption transient and that suppression of the transient in both cases correlates with suppression of the relatively fast phase of •Y122 production strongly implicates the 560 nm absorbing species (as opposed to *X*) as the •Y122-generating intermediate in the rapid phase of the limiting Fe^{2+} reaction. Thus, the SF-Abs data alone imply that different mechanisms are operative.

The EPR and Möss data provide support for this conclusion. Whereas all kinetic data from the excess Fe^{2+} reaction suggest that •Y122 and the diferric cluster are produced simultaneously as the diferric–radical species decays, the data of Figure 6 demonstrate that •Y122 formation precedes diferric cluster formation in the limiting Fe^{2+} reaction. Moreover, broad EPR signals develop only in the limiting Fe^{2+} reaction (not in the limiting Fe^{2+} and ascorbate nor in the excess Fe^{2+} reaction). Conversely, the Mössbauer features attributed to the fast-relaxing ferric species develop only in the excess Fe^{2+} reaction. Thus, data from each of the three methods indicate that the reactions proceed by different mechanisms and are entirely consistent with the two-pathway kinetic scheme (Scheme 1 of paper 1[4]) which we originally proposed.[2]

Identity of the 560 nm Absorbing Species. One aspect of our mechanism with which the data are inconsistent, however, is the identity of the 560 nm absorbing species. Two results demonstrate that the species is not a μ-peroxodiferric cluster. First, no Mössbauer features consistent with this structure are observed. In fact, *no* features can be discerned which correlate temporally (in both development and decay phases) with the 560 nm absorption transient. This result suggests that the 560 nm absorbing species is not iron based. Furthermore, comparison of the RFQ-Möss and SF-Abs data indicates that *X* (which absorbs in the 360 nm region but has no feature at 560 nm) forms concomitantly with development of the absorption transient. This implies that the 560 nm absorbing species and *X* are both components of I and that the absorbing species stores only one of the two oxidizing equivalents of I.

In reconsidering the identity of the 560 nm absorbing species, we have examined the possibility that it is an artifact of the reaction conditions, perhaps involving the buffer. We disfavor this possibility on the basis of several considerations. First, the transient is kinetically competent: it develops rapidly in comparison with the products of the reaction and decays concomitantly with formation of •Y122. Second, development of the transient

(17) Nordlund, P.; Sjöberg, B. M.; Eklund, H. *Nature* **1990**, *345*, 593–598.

(18) Nordlund, P.; Eklund, H. *J. Mol. Biol.* **1993**, *232*, 123–164.

(19) This observation contradicts the report in our previous work[2] that no broad EPR features develop in the reaction of the mutant subunit. Two factors account for our previous failure to recognize these features. First, the R2 concentration employed in our previous work was sixfold lower than that used in the present study. The lower concentration resulted in a poorer signal-to-noise ratio. Second, the broad features decay more rapidly in R2-Y122F than in R2-wt.[14] This trend was not anticipated, since both *X* and the 560 nm absorbing intermediate decay more slowly in R2-Y122F. As a result we failed to examine the optimum time regime to detect the features.

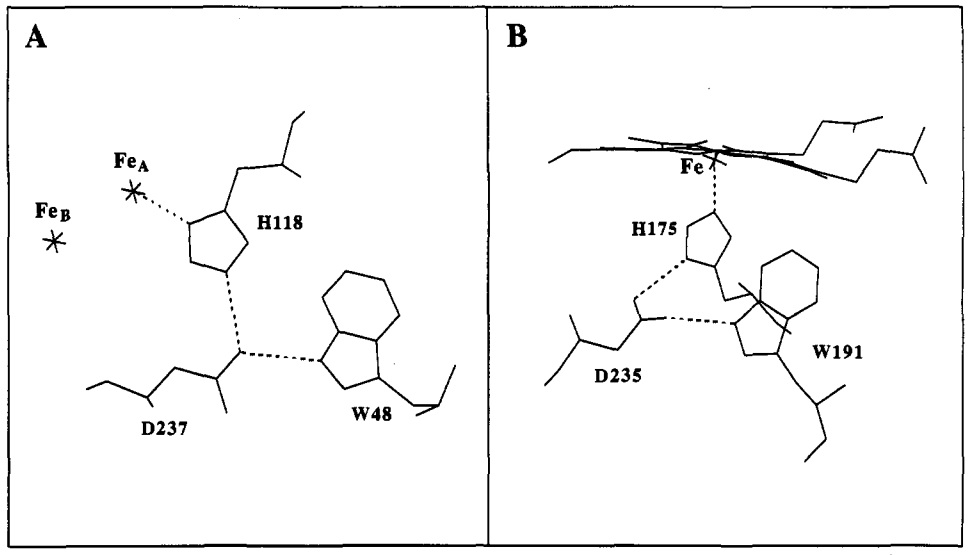

Figure 9. Schematic representation of hydrogen bonding networks (B) in yeast cytochrome *c* peroxidase[29] and (A) in R2[17] which connect a W residue to the active site Fe. Note the different modes of participation of D235 of CcP, which has both oxygens involved in the network, and D237 of R2, which has only a single oxygen involved.

is exquisitely sensitive to the ratio of Fe^{2+}/R2 (but is completely independent of the absolute concentrations of the two). Thus, the transient is not observed in the absence of either Fe^{2+} or apo R2, or when the Fe^{2+}/R2 ratio differs much from 2. Third, the presence of the transient correlates, under all conditions examined, with the presence of a rapid phase of •Y122 production. Finally, the transient is observed when the reaction is carried out in different buffers (e.g. Tris, data not shown). Together, these results suggest that the transient arises from a mechanistically significant intermediate.

As noted above, the absence of Mössbauer features which correlate temporally with the 560 nm transient suggests that the species is not iron based. The observation of broad EPR features at short times in the limiting Fe^{2+} reactions of both R2-wt (Figure 7) and R2-Y122F (Figure 8) suggests that the 560 nm absorbing species may be EPR active. The most likely identity of an oxidizing species, which does not contain iron and is EPR active, is a free radical. Such a radical might be derived either from O_2 or from the protein. For reasons which are enumerated below, our current working hypothesis is that the 560 nm absorbing species is a tryptophan radical cation (•WH^+).[20]

A copious literature exists on the generation of W radicals by pulse radiolysis,[11,21,22] and hence their spectral properties have been defined. This work indicates that the W radical exhibits two absorption bands, with values of λ_{max} which depend on its protonation state.[11,21,22] The neutral tryptophan radical (•W), which is the predominant species in solution at neutral pH (the reported pK_a of the radical cation produced by abstraction of an electron from W is 4.3[22,23]), absorbs maximally at 510 and 325 nm, with molar absorptivities (ϵ_{510} and ϵ_{325}) of 2300 and 3700 M^{-1} cm^{-1}, respectively.[11] The tryptophan radical cation (•WH^+) absorbs maximally at 560 and 335 nm, with molar absorptivities of 3000 and 4750 M^{-1} cm^{-1}, respectively.[11] The λ_{max} values of •WH^+ coincide with the bands observed in the limiting Fe^{2+} reaction, and its ϵ_{560} is similar to that estimated for the 560 nm absorbing species (2500–4800 M^{-1} cm^{-1}).

Second, related work indicates that •W can oxidize tyrosine to a tyrosyl radical.[24-26] •WH^+ should be an even more strongly oxidizing species. Thus, the proposal that the 560 nm absorbing species is a •WH^+ is consistent with the data which suggest that this species generates •Y122 in the fast phase of the limiting Fe^{2+} reaction.

Third, compound I (compound ES) of yeast cytochrome *c* peroxidase (CcP) harbors a radical at W191.[12,27-34] X-ray crystallographic data[35] and biophysical studies of mutant CcP's[36] suggest that this radical is protonated. Not only does the W191 radical exhibit an absorption band centered near 570 nm,[28,37] but it also exhibits a broad, axial, $g = 2.0$ EPR signal.[27] Thus, a •WH^+ might be the origin of the broad features which develop early in the limiting Fe^{2+} reaction of both R2-wt (Figure 7) and R2-Y122F (Figure 8). Furthermore, as pointed out by Nordlund and Eklund, W48 of R2 is related to W191 of CcP. Each is part of a hydrogen bonding network which connects it to its active site iron, and each is near the surface of its protein where it can interact with the relevant electron-donating partner protein (cytochrome *c* for CcP and the R1 subunit for R2).[17,18] In the case of CcP, D235 provides a bridge between N(δ) of H175, the proximal ligand to the heme, and the indole NH of W191 (Figure 9B).[29] In the case of R2, D237 provides a bridge between N(ϵ) of H118, which ligates Fe_A of the diferric cluster, and the indole

(20) In principle, it might be possible to observe the putative tryptophan radical independently of ***X*** by increasing the temperature of the EPR measurement until the electronic relaxation of ***X*** becomes fast and its EPR signal broadens into the baseline. In practice, the presence of isopentane in the RFQ-EPR samples imposes an upper limit of 120 K. At this temperature, the spectrum of ***X*** is broad, but still visible.

(21) Adams, G. E.; Aldrich, J. E.; Bisby, R. H.; Cundall, R. B.; Redpath, J. L.; Willson, R. L. *Radiat. Res.* **1972**, *49*, 278–289.
(22) Posener, M. L.; Adams, G. E.; Wardman, P. *J. Chem. Soc., Faraday Trans. 1* **1976**, *72*, 2231–2239.
(23) Jovanovic, S. V.; Simic, M. G. *J. Free Rad. Biol. Med.* **1985**, *1*, 125–129.
(24) Prütz, W. A.; Butler, J.; Land, E. J.; Swallow, A. *J. Biochem. Biophys. Res. Commun.* **1980**, *96*, 408–414.
(25) Sloper, R. W.; Land, E. J. *Photochem. Photobiol.* **1980**, *32*, 687–689.
(26) Jovanovic, S. V.; Harriman, A.; Simic, M. G. *J. Phys. Chem.* **1986**, *90*, 1935–1939.
(27) Yonetani, T.; Schleyer, H.; Ehrenberg, A. *J. Biol. Chem.* **1966**, *241*, 3240–3243.
(28) Ho, P. S.; Hoffman, B. M.; Kang, C. H.; Margoliash, E. *J. Biol. Chem.* **1983**, *258*, 4356–4363.
(29) Finzel, B. C.; Poulos, T. L.; Kraut, J. *J. Biol. Chem.* **1984**, *259*, 13027–13036.
(30) Edwards, S. L.; Xuong, N. H.; Hamlin, R. C.; Kraut, J. *Biochemistry* **1987**, *26*, 1503–1511.
(31) Mauro, J. M.; Fishel, L. A.; Hazzard, J. T.; Meyer, T. E.; Tollin, G.; Cusanovich, M. A.; Kraut, J. *Biochemistry* **1988**, *27*, 6243–6256.
(32) Erman, J. E.; Vitello, L. B.; Mauro, J. M.; Kraut, J. *Biochemistry* **1989**, *28*, 7992–7995.
(33) Scholes, C. P.; Liu, Y.; Fishel, L. A.; Farnum, M. F.; Mauro, J. M.; Kraut, J. *Isr. J. Chem.* **1989**, *29*, 83–92.
(34) Miller, M. A.; Bandypadhyay, D.; Mauro, J. M.; Traylor, T. G.; Kraut, J. *Biochemistry* **1992**, *31*, 2780–2797.
(35) Wang, J.; Mauro, J. M.; Edwards, S. L.; Oakley, S. J.; Fishel, L. A.; Ashford, V. A.; Xuong, N. H.; Kraut, J. *Biochemistry* **1990**, *29*, 7160–7173.
(36) Fishel, L. A.; Farnum, M. F.; Mauro, J. M.; Miller, M. A.; Kraut, J.; Liu, Y.; Tan, X.; Scholes, C. P. *Biochemistry* **1991**, *30*, 1986–1996.
(37) Coulson, A. F. W.; Erman, J. E.; Yonetani, T. *J. Biol. Chem.* **1971**, *246*, 917–924.

Scheme 3. Current Working Hypothesis for the Mechanism of Assembly of the R2 Cofactor in the Reaction of Apo R2 with Fe^{2+} and O_2[a]

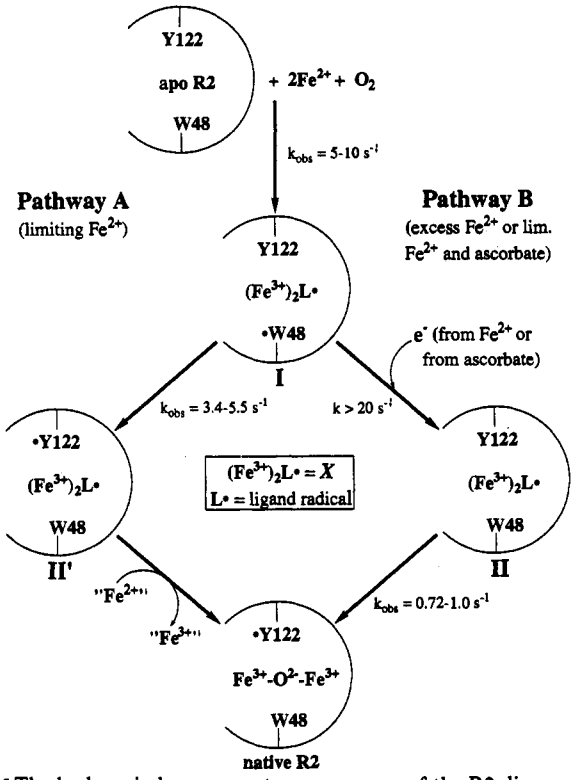

[a] The broken circles represent one monomer of the R2 dimer.

NH of W48 (Figure 9A).[17,18] Thus, the characteristics deduced for the 560 nm absorbing species are all consistent with its being a $^{\bullet}WH^{+}$, and the hydrogen bonding network of which W48 is a part makes it the obvious candidate for the residue which is oxidized. This residue and its H-bonding network were previously proposed to mediate both electron transfer between the two subunits of RNR,[17,18] a step which is thought to be essential in the enzyme's catalytic cycle, and delivery of the extra electron during assembly of the R2 cofactor.[18]

Revised Mechanistic Hypothesis. With the tentative identification of the 560 nm absorbing intermediate as a $^{\bullet}WH^{+}$, both oxidizing equivalents of I are assigned. The complete mechanistic hypothesis which results from this paper and the two preceding it,[4,7] is shown in Scheme 3. This hypothesis is identical with that which we previously put forth, except that the μ-peroxodiferric cluster, which was proposed to be responsible for the 560 nm absorption band,[2] has been eliminated. The available data are still consistent with our previous assertion that neither of the species which generates $^{\bullet}Y122$ is a high valent iron species.[2,3] However, with the current hypothesis that I contains ***X*** and $^{\bullet}WH^{+}$, the participation of a fleeting Fe(IV) species prior to formation of I cannot be ruled out. We can only state that no existing evidence indicates that a ferryl species is involved in the assembly reaction.

Implications of Revised Hypothesis. If the 560 nm absorbing species of intermediate I is, in fact, a radical cation derived from W48, it would provide support for the proposal of Nordlund and Eklund that the residue can function as an electron conduit from the surface of R2 to the cofactor.[18] By virtue of its ability to rapidly reduce a reactive iron/oxygen species, W48 might also serve to direct the outcome of the O_2 activation reaction of R2. W48 may reductively quench a potential 2 e^--oxidizing intermediate species more rapidly than the species can react with other amino acids in its vicinity (including Y122). This one-electron quenching would effectively "split" a two-electron oxidant into two one-electron oxidants ($^{\bullet}WH^{+}$ and ***X***), thus ensuring the desired one-electron chemistry. As proposed in Scheme 3, the fate of the $^{\bullet}WH^{+}$ would then be determined by the availability of reducing equivalents. In the presence of reductant, conditions which should ordinarily prevail *in vivo*, the $^{\bullet}WH^{+}$ would rapidly be reduced, leaving the less accessible ***X*** to generate $^{\bullet}Y122$. In the absence of reductant, $^{\bullet}WH^{+}$ would be reduced (more slowly than in the reductive pathway) by Y122, followed by the even slower reduction of ***X*** by Fe^{2+} to give the product cofactor.

As discussed above, we propose in Scheme 3 that I forms in the excess Fe^{2+} reaction but is reduced too rapidly to accumulate. The basis for depicting I as the branch-point between pathways A and B is the observation that the formation rate constants for I in the limiting Fe^{2+} reaction and for II in the excess Fe^{2+} reaction are equal. It is possible, however, that a precursor to I (rather than I) is rapidly reduced in the excess Fe^{2+} reaction and, therefore, that I does not form. In either case, the relevance of the limiting Fe^{2+} pathway to the reaction as it occurs *in vivo* remains to be established, since small molecules or proteins capable of providing the required electron may be present in the cell. Nevertheless, detailed examination of the reaction carried out under these conditions has allowed the detection of a 560 nm absorbing species, which is possibly a $^{\bullet}WH^{+}$, and which may facilitate delivery of the required extra electron during assembly of the R2 cofactor.

If the proposed $^{\bullet}WH^{+}$ does form in the excess Fe^{2+} reaction and is the site of reduction by Fe^{2+}, it would imply that the extra electron is delivered to different sites in the limiting Fe^{2+} and excess Fe^{2+} reactions. In the excess Fe^{2+} reaction, the extra electron is delivered to the $^{\bullet}WH^{+}$, before $^{\bullet}Y122$ is produced. In contrast, in the limiting Fe^{2+} reaction, the extra electron is delivered to ***X*** at the (buried) cofactor site, after $^{\bullet}Y122$ is produced. Thus, the fate of the Fe^{3+} which results might be expected to differ in the two reactions. Consistent with this suggestion, the "fast-relaxing ferric species", which kinetic evidence implicates as the product of this process in the excess Fe^{2+} reaction, is not detected in the limiting Fe^{2+} reaction. Conversely, the magnetic spectrum characteristic of "adventitiously bound" high-spin ferric ion, which is discernible in the 60 s time-point of the limiting Fe^{2+} reaction, does not develop in the excess Fe^{2+} reaction. These differences, which are observed both in the freeze-quenched samples and in others prepared by exposure of pre-formed ferrous–R2 to O_2 (data not shown), provide additional evidence that the reactions proceed by different mechanisms.

In conclusion, this paper and the two[4,7] which accompany it present kinetic and spectroscopic evidence which suggest (1) that the reconstitution of *E. coli* R2 proceeds by two distinct pathways, (2) that the partition ratio depends on the availability of the "extra" electron, (3) that a different species generates $^{\bullet}Y122$ in each pathway, and (4) that neither $^{\bullet}Y122$-generating species contains Fe(IV). Objectives of our future work will be to structurally characterize the diferric radical species (especially to identify the radical component) and to test our hypothesis that the 560 nm absorbing species is a $^{\bullet}WH^{+}$.

Acknowledgment. We thank Dr. Pär Nordlund for helpful discussions concerning the possibility that the 560 nm absorbing species is a tryptophan radical cation. This work was supported by NIH Grant GM 29595 to J.S. with a supplemental grant to D.E.E. and B.H.H. and by a Whitaker Health Sciences Foundation Fellowship to J.M.B.

Supplementary Material Available: Table of quantities of ***X*** and the diferric cluster as functions of reaction time (1 page). This material is contained in many libraries on microfiche, immediately follows this article in the microfilm version of the journal, and can be ordered from the ACS; see any current masthead page for ordering information.

(38) Atta, M.; Nordlund, P.; Aberg, A.; Eklund, H.; Fontecave, M. *J. Biol. Chem.* **1992**, *267*, 20682–20688.
(39) Fontecave, M.; Gerez, C.; Mansuy, D.; Reichard, P. *J. Biol. Chem.* **1990**, *265*, 10919–10924.